IJCPE
Iraqi Journal of Chemical and Petroleum Engineering

Iraqi Journal of Chemical and Petroleum Engineering
Vol.17 No.4 (December 2016) 113- 123
ISSN: 1997-4884

University of Baghdad
College of Engineering

The Effect of In-situ Stress on Hydraulic Fractures Dimensions

Mohammed Al Humairi[1] and Hassan Abdul Hadi[2]
[1]College of Engineering - Missan University
[2]Petroleum Engineering Department - College of Engineering - University of Baghdad

Abstract
Understanding of in-situ stress profiles and orientations plays a vital role in designing a successful hydraulic fracturing treatment. This paper is an attempet to examine the effect of lithology and in situ stress on geometery of hydraulic fractures. A hydraulic fracturing design simulator software called FracproPT with various capabilities for designing most of hydraulic fracture was used for simulate and optimize the hydraulic fracturing. For studying purpose, three different cases of stress gradient contrast between different formations are considered in this study (0.4, 0.5 and 0.75 psi/ft). The results obtained from the simulator showed that lithologies surrounding the pay zone have an effect on the fracture's height, width, and length. Also, Maximum height is achieved when the stress contrast between the pay zone and the surrounding layers is very small.

Key words: Petroleum, Hydraulic fractures, Stress, Design.

Introduction
Stimulation of oil bearing reservoirs by Hydraulic fracturing included, injection of a high viscosity fracturing fluid down a wellbore at a rate greater than the fluid leak-off rate so that it builds-up pressure to overcome the tensile strength of the reservoir rock and establish an effective communication between the reservoir and the wellbore. The effect is the initiation and propagation of fractures on a plane perpendicular to the least principal stress [1].

Today hydraulic fracturing treatment has extended to involve other applications such as:

- Assisting in secondary and tertiary recovery processes such as water-, fire-, and steam flood operations, to improve injectivity and sweep efficiency.
- Assisting in the injection or disposal of waste water and drill cuttings.
- Bypassing formation damage (skin effect) due to drilling and completion operations by means of a relatively small fracture in order to increase productivity [2].
- Increasing ultimate production from low permeability formations such as tight gas sandstones by means of massive treatments that generate longer fractures than those created for bypassing skin effect.
- Tackling the problem of sand production in poorly consolidated or unconsolidated high permeability formations using coated resin and

reducing wellbore pressure gradient [3].

There are many parameters that controlled the success of this process such as the fracture dimensions – fracture half length, width and height – as well as proppants, fluids, treatment schedule etc.

The fracture geometry then depends on several other factors like in-situ stress fields and modulus contrasts surrounding the formation [4]. The in-situ stress field is a function of geology or the lithological sequence [5].

This paper is an investigation of effect of insitu stresses on design of hydraulic fractures geometry. Three different lithology sequences are considered in this investigation. Fracture geometry is expressed in term length, width, and height. Fracture geometries are modeled in three dimensional with assumption that the reservoir rock is homogeneous, isotropic and linearly elastic. With aid of fracture simulator , a complete analysis of each treatment related to production enhancement, economic estimation are also performed.

Well Data

Table 1 and Figure 1 presented the detailed information of well configuration that being to be fractured.

Table1: Wellbore Configuration

Drilled Hole					
Length (ft)	**Top MD (ft)**	**Bottom MD (ft)**	**Open Hole**	**Bit Diam (in)**	**Effective Diam (in)**
8000	0	2000	Open Hole	14.375	14.375
750	2000	8750	Open Hole	12.250	12.250

Casing						
Length (ft)	**Top MD (ft)**	**Bottom MD (ft)**	**Casing**	**OD (in)**	**Weight (lb/ft)**	**ID (in)**
2000	0	2000	Cemented	13.375	54.500	12.615
8750	0	8750	Cemented	9.625	40.000	8.835

Surface Line/Tubing						
Length (ft)	**Top MD (ft)**	**Bottom MD (ft)**	**Surf Line/Tubing**	**OD (in)**	**Weight (lb/ft)**	**ID (in)**
8500	0	8500	Tubing	3.500	9.30	2.992

Perforation Intervals					
Top MD (ft)	**Bottom MD (ft)**	**Top TVD (ft)**	**Bottom TVD (ft)**	**Diameter (in)**	**Number of Perforations**
8600	8750	8600	8750	0.380	50

Path Summary							
Segment Type	**Length (ft)**	**MD (ft)**	**TVD (ft)**	**Deviation (deg)**	**Ann OD (in)**	**Ann ID (in)**	**Pipe ID (in)**
Tubing	8500	8500	8500	0.00	0.000	0.000	2.992
Casing	100	8600	8600	0.00	0.000	0.000	8.835

Directional Survey						
Build Rate (deg/100 ft)	**Turn Rate (deg/100 ft)**	**DL Sev. (deg/100 ft)**	**MD (ft)**	**Inclination (deg)**	**Azimuth (deg)**	**TVD (ft)**
0.00	0.00	0.00	0.00	0.00	0.00	0.00

Fig. 1: Wellbore Schematic View

Formation Data

Case I

The lithology sequence of this treatment is a dolomite formation (as pay zone with stress gradient of 0.8 psi/ft) surrounded by granite beds from top and bottom(with stress gradient of 1.2 psi/ft). The stress gradient contrast is 0.4 psi/ft. Tables 2 and 3 presents the required data of this lithological sequence.

Case II

The lithology sequence of this treatment is a sandstone formation (as pay zone with stress gradient of 0.5 psi/ft) surrounded by limestone beds from top and bottom (with stress gradient of 1 psi/ft). The stress gradient contrast is 0.5 psi/ft. Tables 4 and 5 presents the required data of this lithological sequence.

Case III

The lithology sequence of this treatment is a sandstone formation (as pay zone with stress gradient of 0.75psi/ft) surrounded by limestone beds from top and bottom (with stress gradient of 1.5 psi/ft).The stress gradient contrast is 0.75 psi/ft. Tables 6 and 7 presents the required data of this lithological sequence.

The mechanical, chemical ,and thermal properties of different layers that included in the study can be shows in Table 8.

Table 2:Reservoir Layer Parameters 1 for case I

Layer	D (ft)	h (ft)	Rock Type	K (mD)	C_t (ft/min$^{1/2}$)	Stress (psi)	Stress Gradient (psi/ft)
1	0.0	8000	Granite	0	0	9600	1.200
2	8000.0	750	Dolomite	2.51e-02	1.860e-04	6700	0.800
3	8750.0	1750	Granite	0	0	10500	1.200

Table 3:Reservoir Layer Parameters 2for case I

Layer	E (psi)	ν	Fracture Toughness (psi·in$^{1/2}$)	Composite Layering Effect	Pay Zone
1	1.0e+07	0.20	1000	25	No
2	1.0e+06	0.25	500	1.00	Yes
3	1.0e+07	0.20	1000	25	No

Table 4: Reservoir Layer Parameters 1 for Case II

Layer	D (ft)	h (ft)	Rock Type	K (mD)	C_t (ft/min$^{1/2}$)	Stress (psi)	Stress Gradient (psi/ft)
1	0.0	8000	Limestone	0	0	8000	1.000
2	8000.0	750	Sandstone	0.0251	1.860e-04	4188	0.500
3	8750.0	1750	Limestone	0	0	8750	1.000

Table 5: Reservoir Layer Parameters 2 for Case II

Layer	E (psi)	ν	Fracture Toughness (psi·in$^{1/2}$)	Composite Layering Effect	Pay Zone
1	3.0e+07	0.30	500	25	No
2	1.0e+06	0.20	1000	1.00	Yes
3	3.0e+07	0.30	500	25	No

Table 6: Reservoir Layer Parameters 1 for Case III

Layer	D (ft)	h (ft)	Rock Type	K (mD)	C_t (ft/min$^{1/2}$)	Stress (psi)	Stress Gradient (psi/ft)
1	0.0	8000	Limestone	0	0	12000	1.500
2	8000.0	750	Sandstone	.0251	1.860e-04	6281	0.750
3	8750.0	1750	Limestone	0	0	13125	1.500

Table 7: Reservoir Layer Parameters 2 for Case III

Layer	E (psi)	ν	Fracture Toughness (psi·in$^{1/2}$)	Composite Layering Effect	Pay Zone
1	3.0e+07	0.30	500	25	No
2	1.0e+06	0.20	1000	1.00	Yes
3	3.0e+07	0.30	500	25	No

Table 8: Phyiscal and Thermal Rock Properties

Rock Type	Specific Gravity	Specific Heat (Btu/lb·°F)	Thermal Conductivity (Btu/ft·hr·°F)
Sandstone	2.65	0.26	2.57
Limestone	2.72	0.21	0.91
Dolomite	2.86	0.21	0.91
Granite	2.7	0.2	1.74

Fracture Fluid Data

As fracturing fluid, SCHLUMBERGER based fluid YF840 HT W/10 LB/K was selected because it has 200 cP apparent viscosity at 40 sec^{-1} (estimated shear rate in the fracture) after about 2 hours of exposure to the reservoir temperature. This was also the first amongst the qualified fluids selected by the FracProPT for the given set of constraints. Fluid loss, thermal properties and cost for YF840 HT W/10 LB/K fluid are presented in Table 9.

Proppant

The selected proppant is 20/40 Arizona Sand, based on the highest fracture conductivity and proppant permeability. Properties of this proppant are presented in Table 10.

Table 9: Fluid Loss, Thermal Properties and Cost for SCHLUMBERGER's YF840 HT W/10 LB/K

Thermal Conductivity	0.320 Btu/ft·hr·°F	**Wall Building Coefficient**	2.45e-04 $ft/min^{1/2}$
Specific Heat	1.00 Btu/lb·°F	**Spurt Loss**	0.0178 gal/ft^2
Specific Gravity	1.000	**Unit Cost**	5 $/gal

Table 10: Properties of 20/40 Arizona Sand (Propant)

Cost	0.05 $/lb	**Diameter**	0.027 in
Bulk Density	100.00 lbm/ft^3	**Proppant Type**	Sand
Packed Porosity	0.426	**Proppant Coating**	None
Specific Gravity	2.79	**Turbulence Coeff a**	1.09
Turbulence Coeff b	0.082		

Results and Discussion

Case I

Figure 2 depicts the variation of fracture dimensions with respect to time. At the beginning of the treatment, width, length and height grow quickly. This can be attributed to the fact that the fracture is growing in the dolomite layer, which has a stress gradient less than the adjacent granite layers. Fracture dimensions are affected by the gradient stresses and depth of the granite layers. Fracture lower height and width below the perforations are smaller than fracture upper height and width above the perforations because the first set is under a higher stress magnitude because of its depth.

In this case of hydraulic fracturing one formation with low stress concentration is located between two formations with a higher stress concentration. As it can be seen in Figure 3, the fracture exhibits its maximum length and width in the middle of the dolomite formation, i.e. the pay zone. On the other hand, fracture conductivity decreases in the pay zone as the distance from the wellbore increases. By the same way, conductivity decreases from the target dolomite layer to the bounding granite layers as one move along the height axis.

Figure 4 shows the concentration of the proppant in the fracture as it relates to fracture length and stress concentration. The major pay zone is a dolomite formation located at 8000 ft. The maximum propagation length is located in the middle of this formation. A fracture length of 1478 ft can be observed. The fracture has a maximum propagation length in the middle where the dolomite formation with the lowest stress concentration is located.

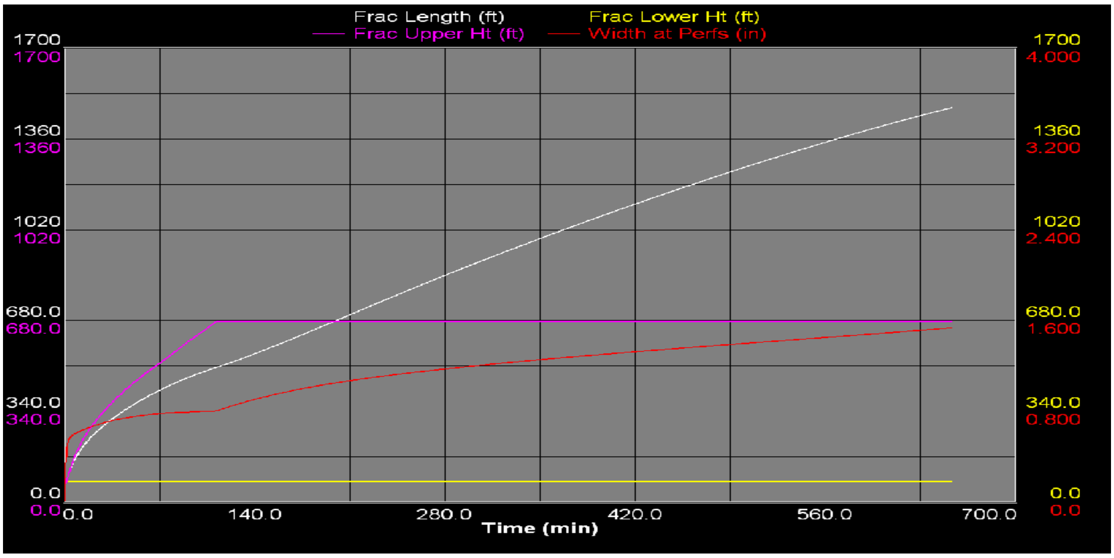

Fig. 2: Fracture Dimensions for Case I

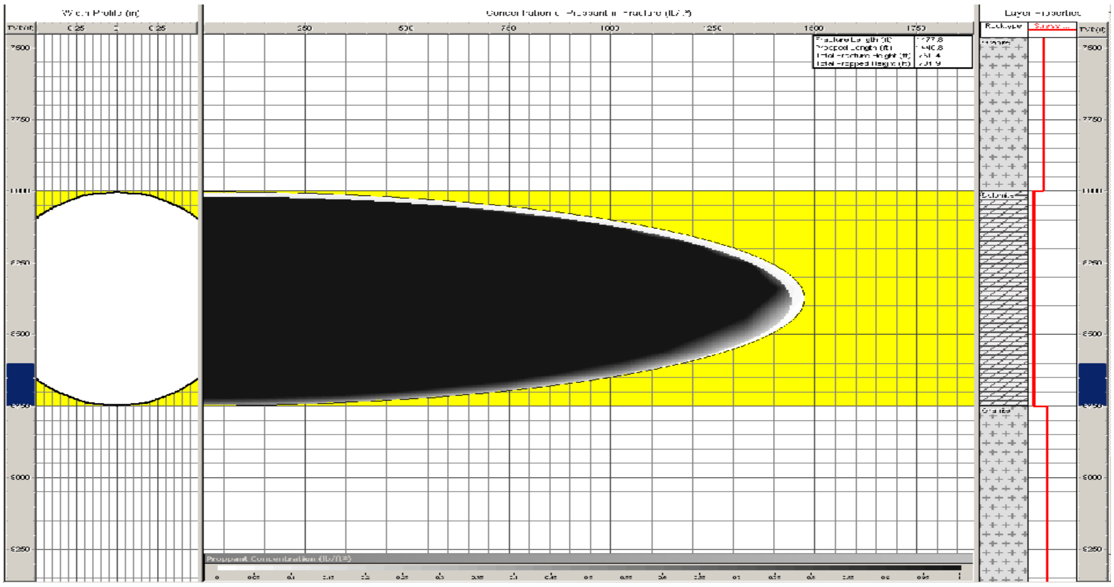

Fig. 3: Fracture Geometry, Width Profile, and Fracture Conductivity for Case I

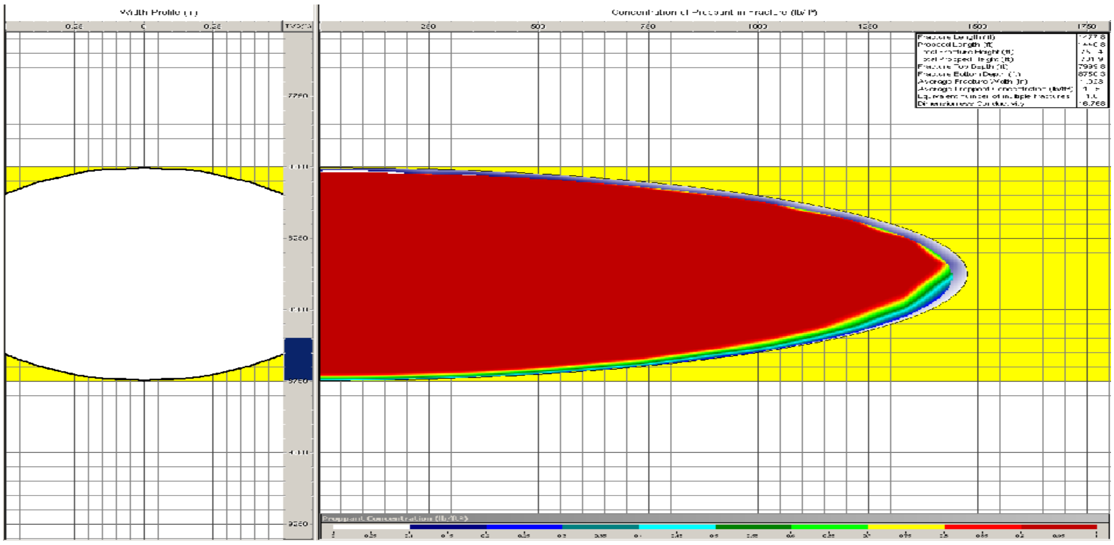

Fig. 4: Fracture Geometry, Width Profile, and Concentration of Proppant in Fracture for Case I

Case II

In Figure 5 the effect of the stress concentration on the fracture propagation can be seen. Figure 5 shows the fracture dimensions as functions of time. All the dimensions increase with increase time, but it can be seen that the fracture grows in length faster than in height or width.

Figure 6 shows the concentration of the proppant in the fracture as it relates to fracture length and stress concentration. The major pay zone is a sandstone formation located at 8000 ft. The maximum propagation length is located in the middle of this formation. A fracture length of 1554 ft can be observed. The fracture has a maximum propagation in the middle where as the sandstone formation with the lowest stress concentration is located.

Figure 7 shows fracture conductivity values inside the fracture with the values decreasing as distance increases from the wellbore to the tip of the fracture along the length axis and also as one move along the height axis away from the sandstone pay zone.

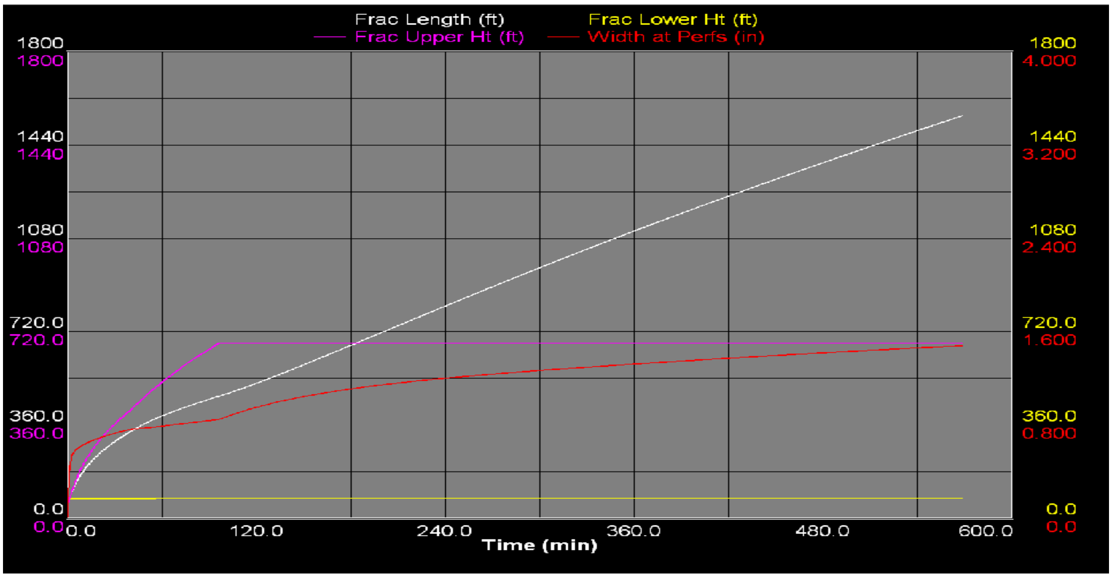

Fig. 5: Fracture Dimensions for Case II

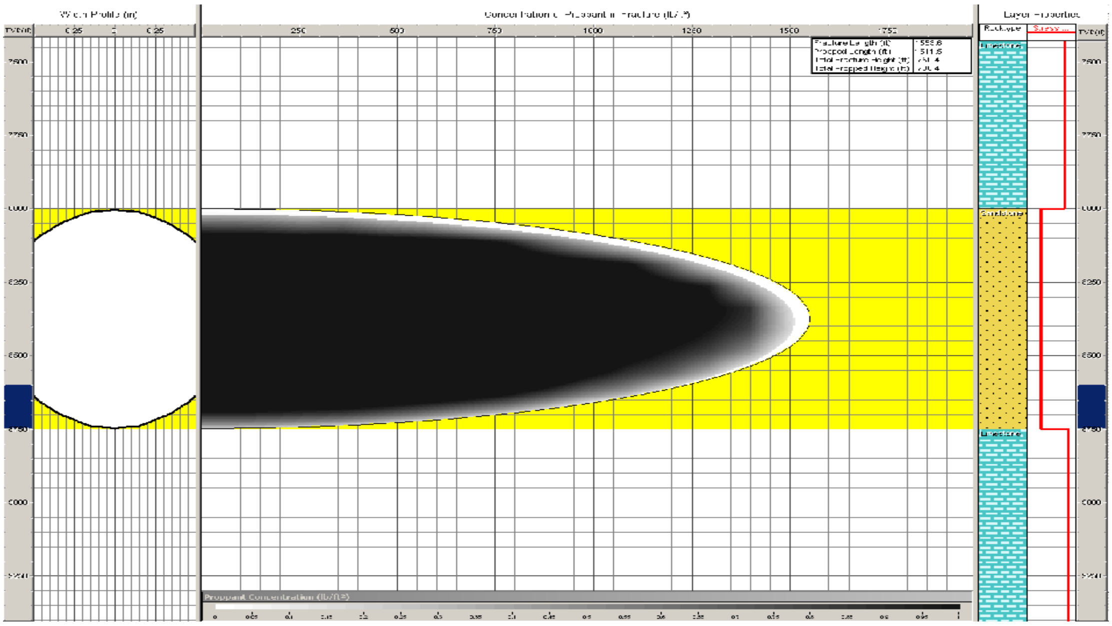

Fig. 6: Fracture Geometry, Width Profile, and Fracture Conductivity for Case II

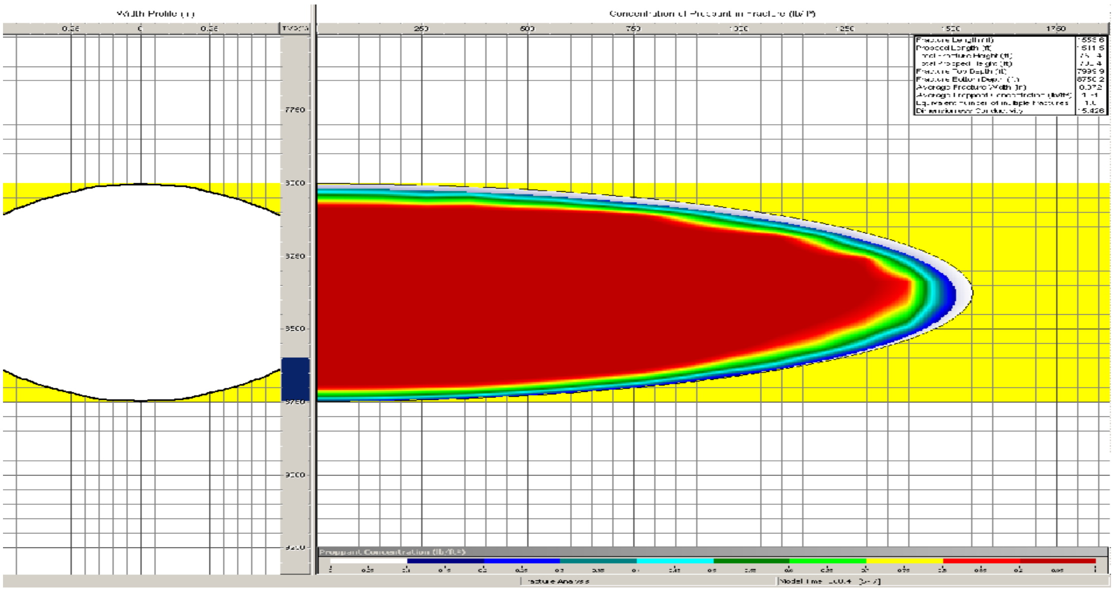
Fig. 7: Fracture Geometry, Width Profile, and Concentration of Proppant in Fracture for Case II

Case III

In Figure 8 the effect of the stress concentration on the fracture propagation can be seen for case III, which has a zero stress gradient. Figure 8 shows the fracture dimensions with respect to time. All the dimensions increase with time. The fracture length however shows more growth compared to the height or width.

Figure 9 shows fracture conductivity values inside the fracture with the values decreasing as distance increases from the wellbore to the tip of the fracture along the length axis and also as one move along the height axis away from the sandstone pay zone.

Figure 10 shows the concentration of the proppant in the fracture as it relates to fracture length and stress concentration. The major pay zone is a sandstone formation located at 8000ft. The fracture has a maximum propagation length n the middle where as the sandstone formation with the lowest stress concentration is located. A fracture length of approximately 1542ft can be observed.

As observed in Table 11 and Figure 11, in-situ stress and young modulus differences between the pay zone and the surrounding formations have an important effect on fracture containment or restriction. We observe that if the young's modulus and the stress gradient of the encompassing layers is greater than the pay zone, it is possible to contain the fracture height within the pay zone.

As for fracture length, case II and case III have same lithology sequence but with different stress gradient contrast between the pay zone and the encompassing layers. Stress gradient contrast in case II is 0.5 psi/ft with fracture length of 1554 ft. Stress gradient contrast in case III is 0.75 psi/ft with fracture length of 1542 ft. These values show small effect of stress contrast on fracture length.

Another observation that related to proppant concentration. The proppant concentration in case II is 1.31 lb/ft^2 with fracture width of 0.97 in, while proppant concentration in case III is 1.63 lb/ft^2 with fracture width of 0.99 in. As result, a small increases in the fracture width is achieved when increasing the proppant concentration in the fracture.

The fracture height in all the cases was 750 ft, which means that the pay zone will be coverage by 100%.

This is due to selection of the right kind of fracturing fluid YF840 HT W/10 LB/K from schlumberger and 20/40 Arizona sand, which gives the highest fracture conductivity and proppant permeability thus giving an optimum output.

Finally, the economic evaluation in term of net present value (NPV) showed the lower value at lower stress gradient contrast (case I) as shown in Table 11. Also the highest NPV value for case II ($86.166B) where the stress gradient contrast is 0.5 psi/ft. Thus, for an optimum treatment, the knowledge of stress differences between the pay zone and the bounding layers play a crucial part.

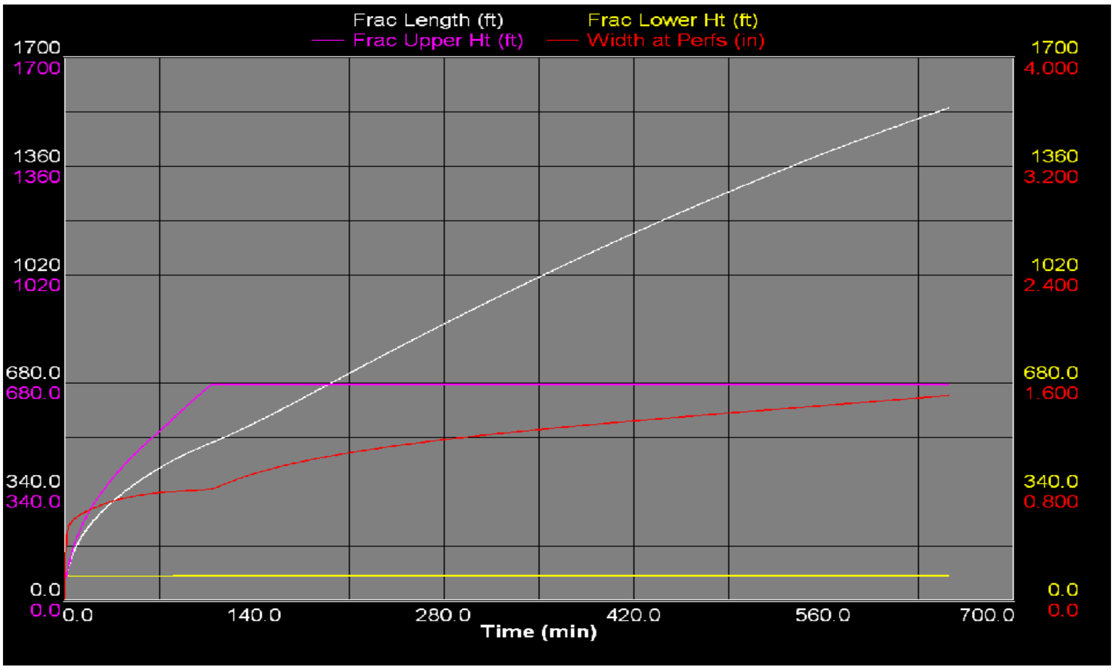

Fig. 8: Fracture Dimensions for Case III

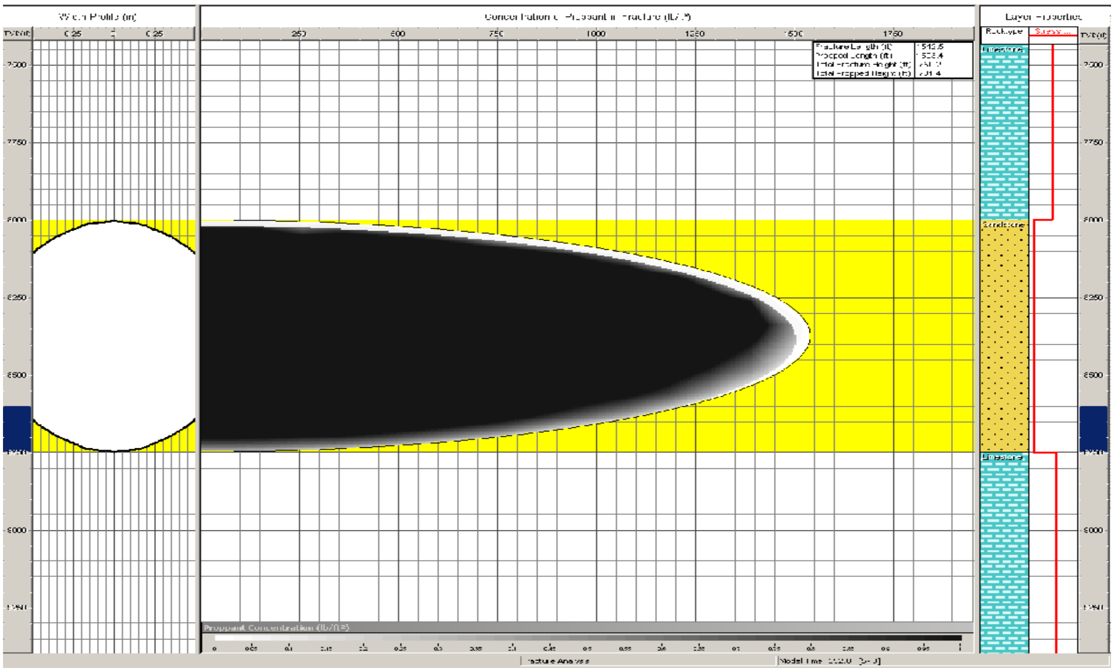

Fig. 9: Fracture Geometry, Width Profile, and Fracture Conductivity for Case III

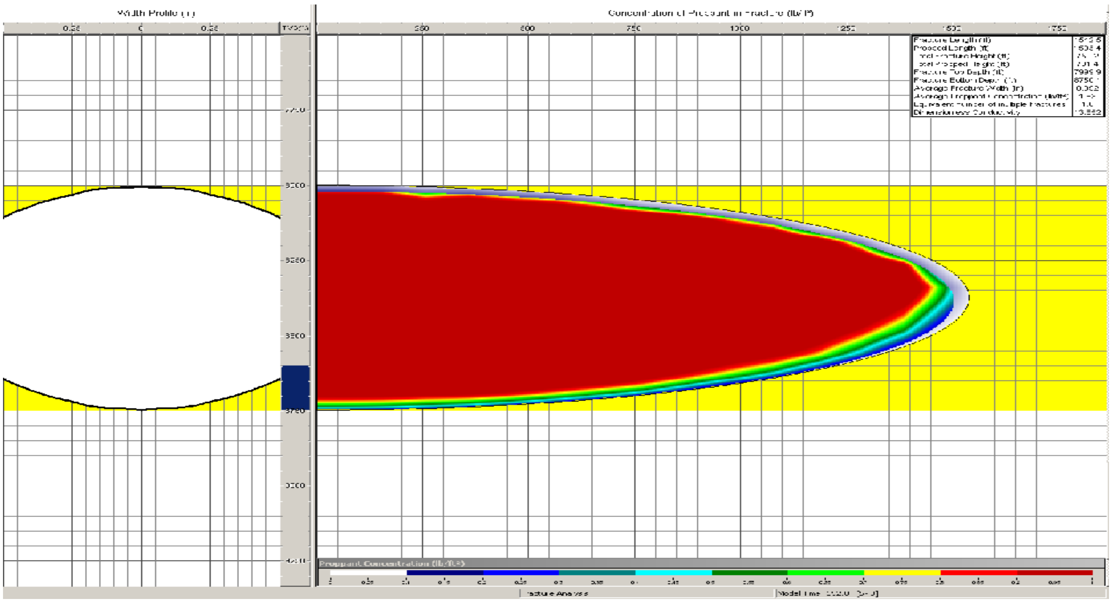

Fig. 10: Fracture Geometry, Width Profile, and Concentration of Proppant in Fracture for Case III

Table 11: Comparison of Results

Fracture Parameters	Case 1	Case 2	Case 3
Stress Gradient (psi/ft)	0.8	0.5	0.75
Stress Gradient Contrast (psi/ft)	0.4	0.5	0.75
Fracture Length (ft)	1478	1554	1542
Propped Length (ft)	1441	1511	1503
Total Fracture Height (ft)	750	750	750
Total Propped Height (ft)	732	730	731
Average Fracture Width (in)	1.02	0.97	0.99
Average Proppant Concentration (lb/ft^2)	1.95	1.31	1.63
Dimensionless Conductivity	16.77	15.36	13.81
NPV (M$)	71397	86166	75330
Cumulative Oil Production (Mbbls)	1576.711	1860.378	1654.363

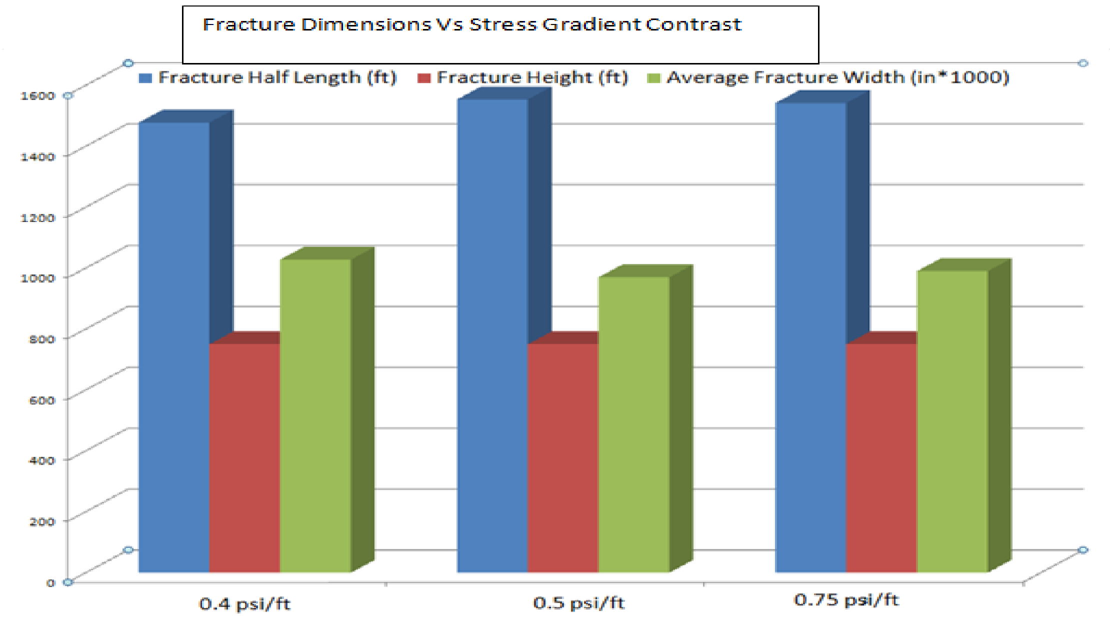

Fig. 11: Results Comparison Plot

Conclusions

Based on the obtained results, the following conclusions are outlined:

1. After analyzing the effect of in-situ stress differences on the fracture geometry, it is clear that this is a crucial factor controlling fracture height, length and width. Stress gradient contrast is responsible for containment or restriction of fracture growth.
2. The selection of a right kind of fracturing fluid and proppant will help you achieve 100% pay zone coverage.
3. The stress gradient contrast between the pay zone and the surrounding layers is inversely proportional to the dimensionless fracture conductivity.
4. Also, the fracture half length increased as the stress gradient decreased.
5. In all the three cases examined , there was good fracture containment as a result of the high young's moduli of the surrounding layers.
6. The net present value (NPV), which is an economic optimization parameter for the treatment design is seen to show some dependence on the stress gradient. Specifically, as the stress gradient increased from 0.5 through 0.75 to 0.8 psi/ft, the NPV decreased from $86.166B, $75.33B and $71.397B respectively.

Nomenclature

E Young's modulus, psi
υ Poisson's ratio, psi
w Width of fracture, in.
L Length of fracture, ft
H Height of fracture, ft
C Leakoff Coefficient, ft/min$^{1/2}$
Ct Total Leakoff Coefficient, ft/min$^{1/2}$
D Size of the tube, in.
K Permeability, mD
ID Internal Diameter, in.
OD Outside diameter, in.
MD Measure Depth, ft
TVD True Vertical Depth, ft
NPV Net Present Value, M$
ROI Rate of Investment, %
PI Productivity Index, dimensionless

References

1. Shah, S. "PE – 5423 Advanced Stimulation Class Notes". MPGE, University of Oklahoma, fall 2008, Norman.
2. FracproPT v10.3.Pinnacle servicesn Help Files, 2007.
3. Zillur Rahim and Mohammed Y. Al-Qahtani. "Sensitivity Study On Geomechanical Properties To Determine Their Impact On Fracture Dimensions And Gas Production In The Khuff And Pre-Khuff Formations Using A Layered Reservoir System Approach, Ghawar Reservoir, Saudi Arabia" SPE paper 72142 prepared for presentation at the SPE Asia Pacific Improved Oil Recovery Conference held in Kuala Lumpur, Malaysia, 8–9 October 2001.
4. R.B. Willis, J. Fontaine, L. Paugh, and L. Griffin. "Geology and Geometry: A Review of Factors Affecting the Effectiveness of Hydraulic Fractures" SPE paper prepared for presentation at the 2005 SPE Eastern Regional Meeting held in Morgantown, M.V., 14-16 September 2005.
5. H. Gu and E. Siebrits. "Effect of Formation Modulus Contrast on Hydraulic Fracture Height Containment" SPE paper prepared for presentation at the 2006 SPE International Oil and Gas Conference and Exhibition in China, Beijing, 5-7 December 2006.
6. E.P. Lolon and M.J. Mayerhofer, Garcia and D.A.Durey, A.C. Byrd and R.D. Rhodes. Integrated Fracture and Production Modeling Study in the Lower Cotton Valley Sands , Northern Louisiana 2008.